OPEN

Neuropsychopharmacology (2013) 38, 1105–1112

www.neuropsychopharmacology.org

Elevating Endogenous GABA Levels with GAT-1 Blockade Modulates Evoked but Not Induced Responses in Human Visual Cortex

Suresh D Muthukumaraswamy*[,1], Jim F M Myers[2], Sue J Wilson[3], David J Nutt[3], Khalid Hamandi[4], Anne Lingford-Hughes[3] and Krish D Singh[1]

[1]CUBRIC, School of Psychology, Cardiff University, Cardiff, UK; [2]Psychopharmacology Unit, School of Social and Community Medicine, University of Bristol, Bristol, UK; [3]Division of Brain Sciences, Centre for Neuropsychopharmacology, Imperial College London, London, UK; [4]The Epilepsy Unit, University Hospital of Wales, Cardiff, UK

The electroencephalographic/magnetoencephalographic (EEG/MEG) signal is generated primarily by the summation of the postsynaptic currents of cortical principal cells. At a microcircuit level, these glutamatergic principal cells are reciprocally connected to GABAergic interneurons. Here we investigated the relative sensitivity of visual evoked and induced responses to altered levels of endogenous GABAergic inhibition. To do this, we pharmacologically manipulated the GABA system using tiagabine, which blocks the synaptic GABA transporter 1, and so increases endogenous GABA levels. In a single-blinded and placebo-controlled crossover study of 15 healthy participants, we administered either 15 mg of tiagabine or a placebo. We recorded whole-head MEG, while participants viewed a visual grating stimulus, before, 1, 3 and 5 h post tiagabine ingestion. Using beamformer source localization, we reconstructed responses from early visual cortices. Our results showed no change in either stimulus-induced gamma-band amplitude increases or stimulus-induced alpha amplitude decreases. However, the same data showed a 45% reduction in the evoked response component at ~80 ms. These data demonstrate that, in early visual cortex the evoked response shows a greater sensitivity compared with induced oscillations to pharmacologically increased endogenous GABA levels. We suggest that previous studies correlating GABA concentrations as measured by magnetic resonance spectroscopy to gamma oscillation frequency may reflect underlying variations such as interneuron/inhibitory synapse density rather than functional synaptic GABA concentrations.
Neuropsychopharmacology (2013) **38,** 1105–1112; doi:10.1038/npp.2013.9; published online 30 January 2013

Keywords: gamma oscillations; alpha rhythm; GABA; tiagabine; evoked responses

INTRODUCTION

The presence and modulation of neuronal responses within specific time and frequency bands has been implicated in the implementation of perception and cognition within the brain. There is also increasing evidence that the most plausible mechanism for the generation of temporally organized network activity is in reciprocally connected neuronal networks containing mixtures of interconnected glutamatergic (excitatory) pyramidal and stellate cells, and GABAergic (inhibitory) interneurons (Bartos *et al*, 2007; Traub *et al*, 1996). However, the neuropharmacological bases of the spatially summated, population-level, neurophysiological responses (both evoked and induced) that are recorded non-invasively in humans with magnetoencephalographic/electroencephalographic (MEG/EEG) are largely unknown.

In a recent observational study we found that, across individuals, the frequency of stimulus-induced network gamma oscillations in primary visual cortex was positively correlated with the concentration of GABA measured with edited magnetic resonance spectroscopy (MRS) (Muthukumaraswamy *et al*, 2009). However, MRS is an indirect measure of synaptic GABA function and could be influenced by a number of anatomical, biochemical/metabolic, or even genetic factors. In this experiment, we wished to test the hypothesis that modulation of endogenous GABA levels would modify either the amplitude or frequency of stimulus-related gamma oscillations in human visual cortex. To do this, we manipulated endogenous GABA levels using the drug tiagabine in a set of healthy control participants in a single-blind crossover design. Tiagabine, used in the treatment of epilepsy, binds with high affinity and selectivity to GABA transporter 1 (GAT-1; Borden *et al*, 1994), the primary GABA reuptake transporter in the human cerebral cortex (Conti *et al*, 2004). GAT-1 transporters are located on both neurons and glia (Minelli *et al*,

*Correspondence: Dr SD Muthukumaraswamy, CUBRIC, School of Psychology, Cardiff University, Park Place, Cardiff, CF10 3AT, UK, Tel: +44 029 207 6455, Fax: +44 029 208 70339,
E-mail: sdmuthu@cardiff.ac.uk
Received 15 October 2012; revised 13 November 2012; accepted 26 November 2012; accepted article preview online 9 January 2013

1995) and their presence at fast-inhibitory $GABA_A$ synapses terminates GABA activity and shapes IPSP activity. The effect of tiagabine, measurable by microdialysis, is to elevate the extracellular/synaptic concentration of GABA (Dalby, 2000; Fink-Jensen *et al*, 1992) and therefore to enhance the actions of endogenous GABA. The electrophysiological effect of tiagabine is to enhance evoked inhibitory postsynaptic current (IPSC) duration without modifying IPSC amplitude (Roepstorff and Lambert, 1994; Thompson and Gahwiler, 1992).

To directly measure neuronal activity in humans, we combined MEG recordings with source estimations using an experimental paradigm that we have previously demonstrated to be highly robust to potentially confounding factors such as day, session, or repetition effects (Muthukumaraswamy *et al*, 2010). MEG is an ideal technique to capture higher frequency oscillations as it is more robust to high-frequency artefact sources such as saccades and neck muscle artefacts than EEG (Fries *et al*, 2008; Whitham *et al*, 2007, 2008; Yuval-Greenberg *et al*, 2008, 2009). The principal hypothesis we tested was that modulation of endogenous GABA levels would modify either the amplitude or frequency of stimulus-related gamma oscillations. Subsidiary to that hypothesis, we tested for GABAergic modulations of several neurophysiological parameters, including stimulus-induced alpha amplitude decreases and evoked response components, which are also known to occur with these stimuli (Muthukumaraswamy *et al*, 2010).

PARTICIPANTS AND METHODS

Participants, Design, and Stimuli

Eighteen right-handed volunteers (14 men and 4 women) participated in the experiment after giving informed consent, with all procedures approved by the UK National Research Ethics Service (South East Wales). Volunteers were screened and excluded for personal histories of neurological and psychiatric disease, current recreational or prescription drug use, and impaired liver function (by standard liver function tests). Early in the data collection, three women volunteers were not able to complete the experiment after becoming too heavily sedated. From this point in the data collection, women were excluded from recruitment, leaving completed data sets from 14 men and 1 woman to analyze (mean age 25.5, range 20–32). All results and conclusions are similar whether this one woman was included/excluded from the analysis. Participants were scanned on 2 separate days, separated by a minimum 7-day washout period, at approximately the same time-of-day. On each day, an initial 'pre' MEG recording was obtained then participants orally ingested a capsule containing either placebo or 15 mg of tiagabine (Gabitril). This oral dose is similar to the 16 mg used in a PET study by Frankle *et al* (2009) and identical to several ongoing imaging studies by our group. Participants were blinded to the contents of the capsule and placebo/control session order was counterbalanced across participants. Following drug/placebo administration, MEG recordings were obtained from participants at 1, 3, and 5-h time-points. At the conclusion of every MEG recording, participants completed several psychological questionnaires including, the Biphasic Alcohol Effects Scale (Martin *et al*, 1993), the Subjective High Assessment Scale (Schuckit, 1980) and asked to qualitatively report their psychological state.

During each MEG recording, participants sat in a magnetically shielded room and were presented with a visual stimulus consisting of a, vertical, stationary, maximum contrast, three cycles per degree, square-wave grating presented on a mean luminance background. The stimulus was presented in the lower left visual field and subtended 8° both horizontally and vertically. A small red fixation square was located at the top right-hand edge of the stimulus and remained on for the entire stimulation protocol (Muthukumaraswamy, 2010; Swettenham *et al*, 2009). The stimulus was presented on a Mitsubishi Diamond Pro 2070 monitor controlled by the Psychophysics Toolbox (Brainard, 1997; Pelli, 1997). The screen size was 1024 by 768 pixels and the monitor frame rate was 100 Hz. The monitor was outside the magnetically shielded room and viewed directly from within, at 2.15 m, through a cut-away portal in the shield. The duration of each stimulus was 1–1.5 s followed by 1.5 s of fixation square only. Participants were instructed to fixate for the entire experiment and, in order to maintain attention, were instructed to 'press the response button as soon as the grating patch disappears'. Responses slower than 750 ms from the termination of the stimulus triggered a visual warning for participants. In each recording session, 120 stimuli were presented and participants responded with their right hand. It took approximately 10 min to complete a session.

MEG Acquisition and Analysis

Whole-head MEG recordings were made using a CTF 275-channel radial gradiometer system sampled at 1200 Hz (0–300 Hz bandpass). An additional 29 reference channels were recorded for noise cancellation purposes and the primary sensors were analyzed as synthetic third-order gradiometers (Vrba and Robinson, 2001). Three of the 275 channels were turned off because of excessive sensor noise. At the onset of each stimulus presentation, a TTL pulse was sent to the MEG system. Participants were fitted with three electromagnetic head coils (nasion and pre-auriculars), which they wore for the entire recording day, and were localized relative to the MEG system immediately before and after the recording session. Each participant had a 1 mm isotropic MRI scan available for source localization analysis. To achieve MRI/MEG co-registration, the fiduciary markers were placed at fixed distances from anatomical landmarks identifiable in participants' anatomical MRIs (tragus, eye centre). Fiduciary locations were verified afterwards using digital photographs.

Offline, data were first epoched from -1 to 1 s around stimulus onset and each trial visually inspected for data quality. Data with gross artefacts, such as, head movements and muscle clenching were excluded from further analysis. Reaction times were calculated for each trial relative to the (variable) offset of each grating stimulus. Any trial where there was no behavioural responses or a response >750 ms were classified as incorrect responses and excluded from further analysis. For each participant, we ensured that equal number of trials, from each recording was used in the analysis. To achieve this, trials were removed from the end

of each recording run so that each participant had an equal number of trials submitted for each condition in the analysis. Following these trial removal procedures, the mean number of trials remaining to analyze was 105.5 per participant (range 82–117).

Three source localizations were performed on each data set using synthetic aperture magnetometry (Robinson and Vrba, 1999), one for gamma (30–80 Hz), one for alpha (8–15 Hz), and one for evoked responses (SAMerf; Robinson, 2004). Correspondingly, three global covariance matrices were calculated for each data set, one for gamma, one for alpha, and one for SAMerf (0–100 Hz). Based on these covariance matrices, using the beamformer algorithm (Robinson and Vrba, 1999), three sets of beamformer weights were computed for the entire brain at 4 mm isotropic voxel resolution. A multiple local-spheres (Huang *et al*, 1999) volume conductor model was derived by fitting spheres to the brain surface extracted by FSL's Brain Extraction Tool (Smith, 2002). Readers unfamiliar with SAM are referred to several methodological reviews (Hillebrand *et al*, 2005; Vrba and Robinson, 2001).

For gamma-band SAM image reconstruction virtual sensors were constructed for each beamformer voxel and Student's *t*-images of source power changes computed using a baseline period of -1 to 0 s and an active period of 0 to 1 s, while for alpha-band SAM image reconstruction a baseline period of -1 to -0.3 s and an active period of 0.3 to 1 s was used. This latter time window was used to avoid confounding alpha responses with the time-locked evoked response. After generating the source reconstruction images, the voxel with the strongest power increase (in the contralateral occipital lobe) was located for gamma and the voxel with the strongest source power decrease located for alpha. The source analysis and peak voxel identification procedures were carried out separately for each recording as participants were moved in and out of the MEG between recordings, which would alter their head position in the MEG dewar. To reveal time-frequency responses at these locations, the virtual sensors at these locations were repeatedly band-passed filtered between 1 and 160 Hz at 0.5 Hz frequency step intervals, filtering with an 8 Hz bandpass, third-order Butterworth filter (Le Van Quyen *et al*, 2001; Muthukumaraswamy *et al*, 2010). The Hilbert transform was used to obtain the amplitude envelope and time-frequency spectra were computed as a percentage changed from the pre-stimulus baselines for each frequency band. From these spectra, the peak frequency and amplitude at that frequency for late gamma amplitude increases (30–80 Hz, 0.3–1 s), early gamma amplitude increases (30–150 Hz, 0.05–0.1 s), and alpha amplitude decreases (8–15 Hz, 0.3–1 s) were quantified by collapsing across the time dimension and finding the maximal (or minimal for alpha) frequency. We also checked for confounding effects of using relative change baselines by computing the average absolute values of the source amplitude estimates within the respective time-frequency bins.

For SAMerf, the computed evoked response was passed through the 0–100 Hz beamformer weights to generate SAMerf images (Robinson, 2004) at 10 ms intervals from 50–150 ms. The image window (usually 70–80 ms or 80–90 ms) with the maximal response in visual cortex was identified and the maximal voxel selected as the peak location for further analysis. For this, the evoked field was computed for this virtual sensor (-0.2 to 0-s baseline) and the peak amplitude and latency of the M80 and M150 responses quantified.

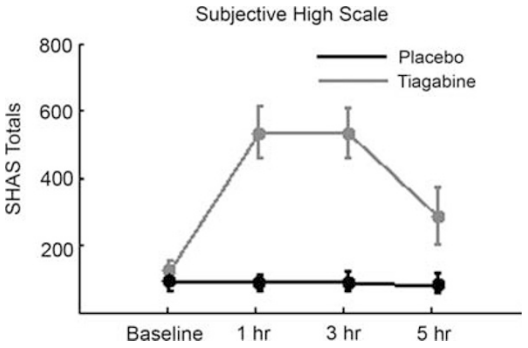

Figure 1 Summary of total scores for participants on the subjective high assessment scale (Schuckit, 1980). The maximum score on this scale is 1300 but varies according to participants' subjective interpretation of the instruction set.

For the production of grand-average SAM maps, individual SAM images were first spatially normalized onto the MNI (T1) average brain using FMRIB's Linear Affine Registration Tool (Jenkinson and Smith, 2001). This was done by first obtaining a set of warping parameters by registering the participant's anatomical MRI with the average brain and then applying these parameters to the SAM source power maps. The grand-average images presented in Figure 2 are the grand-average across both participants and conditions.

All statistical analyses were performed with a 2×4 repeated-measures ANOVA. For these analyses, there were main effects of 'day', 'session', and an interaction term 'drug', presented in that order. Here, the critically important term is the interaction term, indicative of a tiagabine drug-effect. It should be noted that for $F_{(1, 14)}$ the critical value is 4.6 and for $F_{(3, 42)}$ the critical value is 2.82 (alpha = 0.05). Standard errors are used to express variance throughout.

RESULTS

Figure 1 shows summed scores from the subjective high assessment scale (Schuckit, 1980) that participants completed at the end of each recording session. This demonstrates that participants were subjectively strongly affected by tiagabine. Individual items that showed the largest increase relative to placebo were 'feeling of intoxication', 'dizziness', and 'drug effect is like alcohol'. Task response accuracy data showed a significant interaction effect ($F_{(1, 14)} = 3.71$, $F_{(3, 42)} = 2.34$, $F_{(3, 42)} = 2.99$, $p < 0.041$) with *post hoc* testing showing a weak effect at 3 h for the tiagabine session to have more errors (tiagabine 94.9(2.1) %, placebo 98.5(0.6) %, $t_{(14)} = 2.99$, $p = 0.06$). Reaction time data showed a main effect of day and an interaction effect ($F_{(1, 14)} = 12.7$, $p < 0.003$, $F_{(3, 42)} = 0.73$, $F_{(3, 42)} = 3.11$, $p < 0.036$). *Post hoc* tests showed reaction times were significantly slowed at 3 h (tiagabine 271(17) ms, placebo 215(13) ms, $t_{(14)} = 4.719$, $p < 0.001$) and 5 h (tiagabine 251(20) ms, placebo 208(14) ms, $t_{(14)} = 3.733$, $p < 0.002$) after tiagabine.

Figures 2a–c show grand-averaged source reconstructions for gamma-band (30–80 Hz), alpha-band (8–15 Hz) and

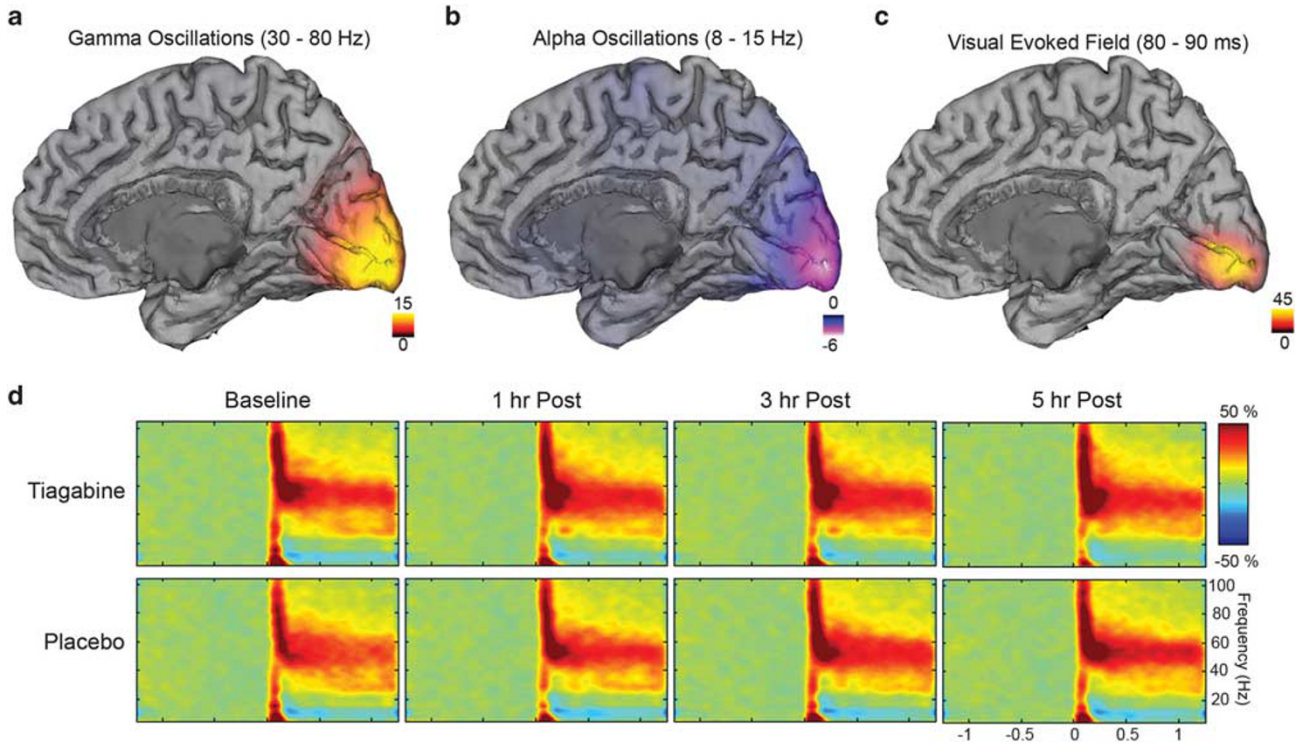

Figure 2 (a–c) Grand-averaged source localization of gamma oscillations (30–80 Hz), alpha oscillations (8–15 Hz), and the visual evoked response (80–90 ms). Units are *t*-statistics for panels a, b, and arbitrary units for panel c. The peak source location for the gamma-band was at Talairach co-ordinate [13, −99, −1], [21, −97, −1] for the alpha-band and [15, −89, 1] for the evoked field. Note: in these beamformer images spatial extent of the colour map does not represent the spatial extent of 'activation' (see Barnes and Hillebrand, 2003). (d) Grand-averaged time-frequency spectrograms showing source-level (gamma peak location) oscillatory amplitude changes following visual stimulation with a grating patch (stimulus onset at time = 0). Spectrograms are displayed as percentage change from the pre-stimulus baseline. Spectrograms were computed for frequencies up to 160 Hz but truncated here to 100 Hz for visualization purposes.

evoked field (80–90 ms) responses to presentation of the grating stimulus and as previously reported (Brookes *et al*, 2005) these are generated in the medial visual cortex in the hemisphere opposite to the side of visual stimulation and closely colocalized. The spatial separation of the peak locations from each other was approximately 1 cm. Time-frequency analyses for the gamma-band locations are presented in Figure 2d, grand-averaged for each day and recording session, and show the typical component morphology following this type of visual stimulus. There is an initial transient broadband (50–100 ms) amplitude increase in the gamma-frequency (>30 Hz) band ('early gamma'), followed by a longer-lasting elevation of gamma-frequency amplitude in a narrower frequency range ('late gamma'). In the lower frequencies, there is an initial transient onset response, which is a characteristic signature of the evoked response (Clapp *et al*, 2006; Muthukumaraswamy *et al*, 2010; Swettenham *et al*, 2009), followed by a sustained alpha amplitude decrease.

Response components were parameterized (using the optimal virtual sensor locations for each component) for each participant and subjected to statistical analysis (Figure 3). Neither early gamma frequency ($F_{(1,14)} = 0.093$, $F_{(3,42)} = 2.17$, $F_{(3,42)} = 0.73$) or late gamma frequency ($F_{(1,14)} = 1.42$, $F_{(3,42)} = 1.16$, $F_{(3,42)} = 1.70$) showed any significant effects. Similarly, neither early gamma amplitude ($F_{(1,14)} = 0.23$, $F_{(3,42)} = 0.25$, $F_{(3,42)} = 1.57$) or late gamma amplitude ($F_{(1,14)} = 0.02$, $F_{(3,42)} = 2.24$, $F_{(3,42)} = 1.55$) demonstrated any effects. Alpha activity showed some non-drug specific effects including, alpha frequency showing a main effect of session but no interaction effect ($F_{(1,14)} = 2.32$, $F_{(3,42)} = 3.58$, $p < 0.03$, $F_{(3,42)} = 0.53$), while alpha amplitude showed a main effect of day effect but no interaction effect ($F_{(1,14)} = 7.78$, $p < 0.02$, $F_{(3,42)} = 0.46$, $F_{(3,42)} = 0.93$). In addition, we performed similar statistical analyses on the individual time-frequency 'pixels' to look for subtle time-frequency effects (data not shown) and these demonstrated similar null effects. Finally, we checked to see if there were any confounding effects of using relative change baselines by extracting absolute amplitude values (no baselining performed) for the various time-frequency windows. For gamma, no effects were seen for the early ($F_{(1,14)} = 3.57$, $F_{(3,42)} = 0.87$, $F_{(3,42)} = 0.14$), late ($F_{(1,14)} = 3.30$, $F_{(3,42)} = 0.15$, $F_{(3,42)} = 0.26$), or baseline periods ($F_{(1,14)} = 1.05$, $F_{(3\ 42)} = 0.08$, $F_{(3,42)} = 0.21$). For alpha, no effects were seen in the active ($F_{(1,\ 14)} = 3.98$, $F_{(3,42)} = 1.41$, $F_{(3,42)} = 0.67$) or the baseline period ($F_{(1,14)} = 0.15$, $F_{(3,42)} = 0.08$, $F_{(3,42)} = 0.14$).

In Figure 4, the source-level evoked responses are presented for both tiagabine and placebo. These demonstrate a clear reduction in the amplitude of the first evoked response component that occurs just after 80 ms (labeled 'M80') following tiagabine and an enhanced second component (labeled 'M150'). Statistical analysis of the M80 amplitudes data showed a main effect of day, session, and critically an interaction effect ($F_{(1,14)} = 24.7$, $p < 0.001$,

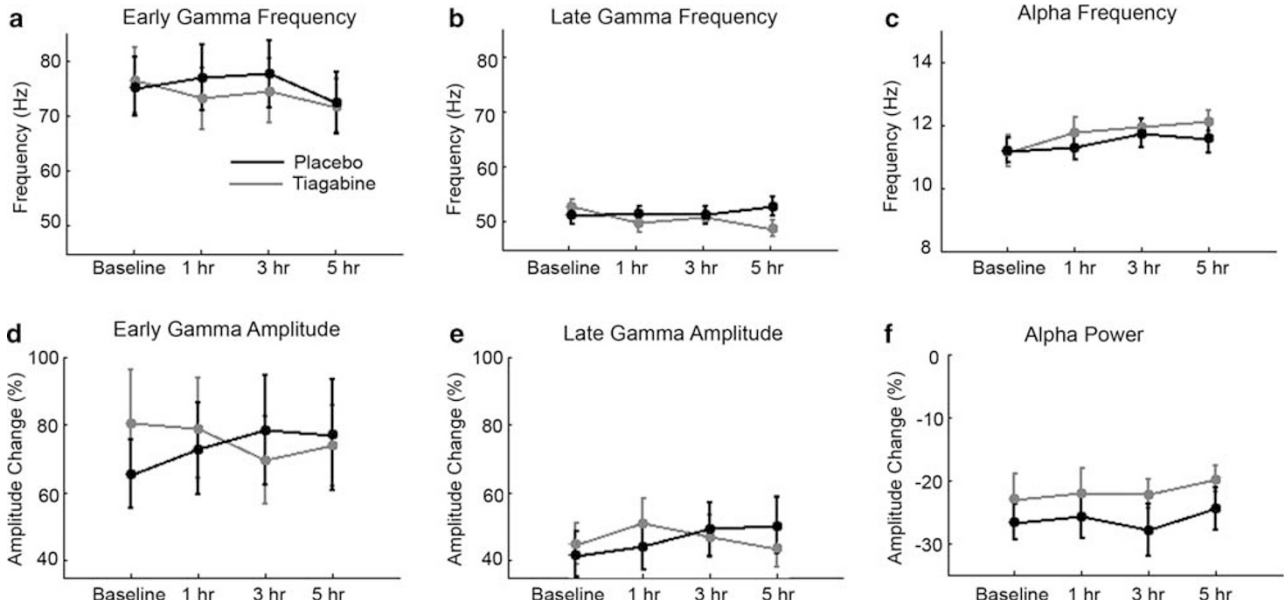

Figure 3 Summary of the experimental time courses of oscillatory time-frequency parameters (a–f) in early visual cortex for both tiagabine and placebo sessions. Early gamma was defined in the range 30–150 Hz, 0.05–0.1 s, late gamma was defined in the range 30–80 Hz, 0.3–1 s, and alpha in the range 8–15 Hz, 0.3–1 s. No oscillatory parameters displayed an interaction effect indicative of a drug effect.

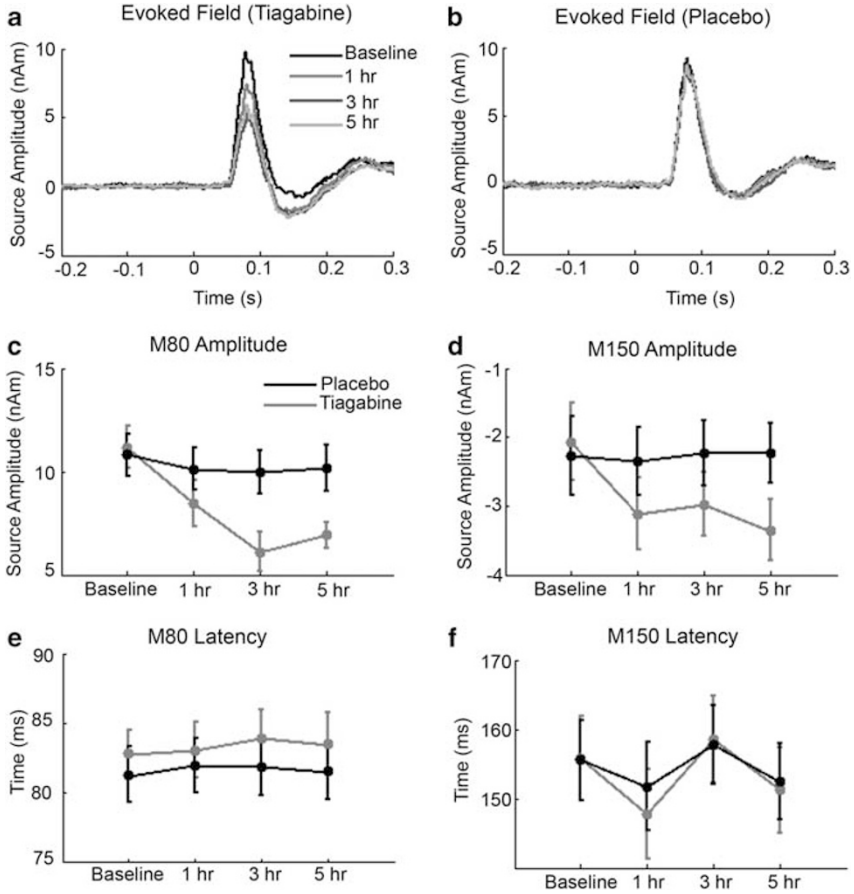

Figure 4 Source-level evoked field analysis for tiagabine (a) and placebo (b). Extracted M80 and M150 amplitudes are presented in (c) and (d), respectively. Both these parameters showed significant interaction effects; indicating an effect of drug. Note: the negative scaling of (d). The peak latencies of these responses are summarized in (e) and (f), respectively. These did not show significant interaction effects.

$F_{(3,42)} = 30.9$, $p < 0.001$, $F_{(3,42)} = 13.1$, $p < 0.001$). M150 amplitudes showed significant effects of day, session, and an interaction effect ($F_{(1,14)} = 7.26$, $p < 0.001$, $F_{(3,42)} = 3.60$, $p < 0.03$, $F_{(3,42)} = 4.00$, $p < 0.02$). The M80 latency showed a day effect but no other effects ($F_{(1,14)} = 8.06$, $p < 0.02$, $F_{(3,42)} = 0.49$, $F_{(3,42)} = 0.14$) and M150 latency showed no significant effects ($F_{(1,14)} = 0.14$, $F_{(3,42)} = 2.34$, $F_{(3,42)} = 0.35$). No correlations were observed between the SHAS measures or reaction times and the evoked field magnitudes and their respective change from baseline scores.

Finally, we conducted an analysis to check whether there were any systematic differences in virtual sensor locations that might potentially have confounded the results. The virtual sensor locations for gamma, alpha, and evoked response locations were tested using ANOVA in X, Z, and Z directions. No significant interaction effects were observed, indicating no systematic changes in response locations with tiagabine.

DISCUSSION

In the current experiment, we elevated endogenous GABA in human participants by administering the GAT-1 blocker tiagabine, while measuring evoked and induced visual responses with MEG. The data showed a clear modification of visual evoked responses but, contrary to our hypotheses, we found no alteration in stimulus-induced oscillatory responses in either the alpha or gamma-frequency bands. We believe our approach did significantly increase GABA based on previous PET studies using a similar dose of tiagabine that show GABA-related changes in tracer binding (Frankle *et al*, 2009, 2012; Myers *et al*, 2012).

One particularly striking feature of the dissociation between evoked and induced responses is that this occurred in the same temporal segments of MEG data. That is, there was a clear reduction in the M80 evoked response but no alteration in the temporally congruent early gamma spike (50–100 ms). This suggests that these two MEG responses have different generator mechanisms. The early gamma response may reflect early ascending input from the lateral geniculate nucleus (Castelo-Branco *et al*, 1998) and is manifested across all cortical layers, although particularly in layers II and III (Xing *et al*, 2012), whereas early evoked responses are mostly generated in layer IV (Kraut *et al*, 1985). The pharmacological basis of this selective modulation presumably lies in the complex distribution of $GABA_A$ and $GABA_B$ receptor subunits across the lamina of V1 (Hendry *et al*, 1994; Zilles *et al*, 2004). In particular, the inhibition provided by $GABA_A$ activation is thought to control response gain to stimuli in primary visual cortex (Katzner *et al*, 2011) and to control the layer-specific spread of excitatory activity caused by visual stimulation (Olivas *et al*, 2012). Reduction of this horizontal spread of excitation (decreased spatial summation) during stimulation onset may be the mechanism underlying the diminished evoked responses we have observed.

This selective modulation also suggests other more-simplistic interpretations of the data are incorrect. For example, one might argue that the reduction in M80 amplitude is due to reduced task vigilance, attention, or even fixation control as participants changed psychological state after tiagabine ingestion. However, each of these explanations would also be expected to modulate oscillatory gamma amplitude (Hoogenboom *et al*, 2010; Kahlbrock *et al*, 2012). Similarly, as these dissociable parameters are all based on the same data, they all have the same relative signal-to-noise ratio. The 45% peak reduction we observed in M80 amplitude is significantly larger than other studies examining visual evoked potentials (VEPs) with benzodiazepenes that affect GABAergic function. In all, 20 mg diazepam administered intravenously (Loughnan *et al*, 1987) or 10 mg administered orally (Bartel *et al*, 1988) has no effect on the VEP. However, 6 and 12 mg of the benzodiazepine bromazepam has been shown to reduce ERP components beginning with the N1 (Bauer *et al*, 1997) and 10 μg/kg of intravenous midazolam caused a relatively small reduction in N75-P100 amplitude (van Leeuwen *et al*, 1992). In fact, it has been shown that tiagabine, which increases GABA rather than acting via the benzodiazepine receptor, actually increases the amplitude of early somatosensory evoked potential components (Restuccia *et al*, 2002). The lack of correlation between the subjective measures in the SHAS and evoked field changes suggest that the changes in evoked field are not simply attributable to the arousal state of participants. Another possibility is that the decreased evoked responses we observed might be due to decreased fixation control during the tiagabine-affected conditions. However, loss of fixation control might be expected to alter the response location of both retinotopic evoked responses (Di Russo *et al*, 2002) and also gamma-band responses as these are retinotopically organized (Perry *et al*, 2011). Our analysis of source peak activity locations indicated no shifts in spatial location for either of these response components. Further, the amplitude of gamma-band activity is very sensitive to the retinotopic position of the stimulus and falls off more rapidly with eccentricity (Swettenham *et al*, 2009) than evoked components. Our gamma-band amplitudes remained unaltered across conditions. Nevertheless, measurement of fixation position via either eye-tracking or electrooculography would be a useful addition to future experiments.

Direct manipulation of GABA levels in this experiment does not appear to have altered gamma frequency, and potential reasons for this are worth considering. It is possible that the lack of effect in the oscillatory domain is due to a lack of statistical power, or perhaps because an inadequate dose of tiagabine was given. However, we do not believe that it would be ethically or feasibly possible to give a much higher dose to control participants and still have them complete the required tasks given the profound behavioural and subjective effects on participants. We also note that overall data quality was very high, with gamma activity identifiable in every subject. Further, although there is no guarantee that raising GABA levels with this dose of tiagabine has a direct effect on the synaptic (eg, time constants) properties of neurons in visual cortex, this is unlikely since similar doses have been shown to change 11C-flumazenil and 11C-Ro15 4513 binding potentials (Frankle *et al*, 2009, 2012; Myers *et al*, 2012). In addition, tiagabine-induced increases in GABA could potentially

modulate GABAergic synapses on all neuronal subtypes, including pyramidal cells and inhibitory interneurons, and receptor subtypes ($GABA_A$ (six subtypes) and $GABA_B$) with unpredictable effects on oscillatory dynamics until the role of all these GABA receptors is elucidated.

In a previous study we found, across individuals, that the frequency of stimulus-induced network gamma oscillations in primary visual cortex was positively correlated with the concentration of GABA measured with MRS. MRS measures the total bulk of GABA in a given area of the brain (usually from a rather large voxel, eg, 27 cm^3). Consistent with invasive evidence, MRS returns concentrations of GABA in the millimolar range (Puts and Edden, 2012). In the synaptic cleft, GABA concentration can reach the millimolar range (Mody *et al*, 1994) but this rapidly declines (<1 ms). Although estimates for ambient levels GABA in the extracellular space range from tens of nanomolar to micromolar (Farrant and Nusser, 2005) these are still orders of magnitude less than the total bulk of GABA. Therefore, MRS measures of GABA concentration probably depend on interneuron numbers/inhibitory synapse numbers, and/or the rate constants of glutamic acid decarboxylase, GABA transaminase, and GAT-1. In particular, interneuron density/synapse numbers, which are inherently structural parameters (Schwarzkopf *et al*, 2012), would not be susceptible to short-term pharmacological manipulations, as we have attempted here.

Although our specific hypothesis was not confirmed, the data here are promising for the relatively unexplored field of pharmaco-MEG (Hall *et al*, 2010). We note another very recent study using the cholinergic agonist physostigmine found a selective modulation of alpha oscillation amplitude (but not gamma) in response to visual stimuli in humans with MEG (Bauer *et al*, 2012). These studies therefore demonstrate that MEG can noninvasively characterize the effect of pharmacologically targeted and physiologically selective agents using alterations in quantitative neuronal biomarkers. Future studies systematically investigating the pharmacological sensitivity of MEG responses will allow the development of data-driven pharmacological models of these responses. Given the wide range of safe and selective interventional agents that can be safely administered to interact with neurotransmitter systems, this bodes well for our future understanding of the neuropharmacological basis of MEG/EEG.

DISCLOSURE

Professor Lingford-Hughes has received honoraria from Janssen-Cilag, Pfizer, Servier, Lundbeck, and from the British Association for Psychopharmacology. She has provided consultancy to NET Device, received research funding from Archimedes, Lundbeck, Pfizer, and Schering, and holds research grants with GlaxoSmithKline. Professor Nutt has performed consultancies for GSK, BMS, Lilly Janssen, Servier, and Lundbeck with additional speaking honoraria from Reckitt-Benkiser. Professor Nutt has worked for UK Government's Committee on Safety of Medicines, The Advisory Council on the Misuse of Drugs and the British National Formulary. The remaining authors declare no conflict of interest.

REFERENCES

Barnes GR, Hillebrand A (2003). Statistical flattening of MEG beamformer images. *Hum Brain Mapp* **18**: 1–12.

Bartel P, Blom M, van der Meyden C, de Klerk S (1988). Effects of single doses of diazepam, chlorpromazine, imipramine and trihexyphenidyl on visual-evoked potentials. *Neuropsychobiology* **20**: 212–217.

Bartos M, Vida I, Jonas P (2007). Synaptic mechanisms of synchronized gamma oscillations in inhibitory interneuron networks. *Nat Rev Neurosci* **8**: 45–56.

Bauer LO, Gross JB, Meyer RE, Greenblatt DJ (1997). Chronic alcohol abuse and the acute sedative and neurophysiologic effects of midazolam. *Psychopharmacology (Berl)* **133**: 293–299.

Bauer M, Kluge C, Bach D, Bradbury D, Heinze HJ, Dolan RJ *et al* (2012). Cholinergic enhancement of visual attention and neural oscillations in the human brain. *Curr Biol* **22**: 397–402.

Borden LA, Murali Dhar TG, Smith KE, Weinshank RL, Branchek TA, Gluchowski C (1994). Tiagabine, SK&F 89976-A, CI-966, and NNC-711 are selective for the cloned GABA transporter GAT-1. *Eur J Pharmacol* **269**: 219–224.

Brainard DH (1997). The psychophysics toolbox. *Spat Vis* **10**: 433–436.

Brookes MJ, Gibson AM, Hall SD, Furlong PL, Barnes GR, Hillebrand A *et al* (2005). GLM-beamformer method demonstrates stationary field, alpha ERD and gamma ERS co-localisation with fMRI BOLD response in visual cortex. *Neuroimage* **26**: 302–308.

Castelo-Branco M, Neuenschwander S, Singer W (1998). Synchronization of visual responses between the cortex, lateral geniculate nucleus, and retina in the anesthetized cat. *J Neurosci* **18**: 6395–6410.

Clapp WC, Muthukumaraswamy SD, Hamm JP, Teyler TJ, Kirk IJ (2006). Long-term enhanced desynchronization of the alpha rhythm following tetanic stimulation of human visual cortex. *Neurosci Lett* **398**: 220–223.

Conti F, Minelli A, Melone M (2004). GABA transporters in the mammalian cerebral cortex: localization, development and pathological implications. *Brain Res Brain Res Rev* **45**: 196–212.

Dalby NO (2000). GABA-level increasing and anticonvulsant effects of three different GABA uptake inhibitors. *Neuropharmacology* **39**: 2399–2407.

Di Russo F, Martinez A, Sereno MI, Pitzalis S, Hillyard SA (2002). Cortical sources of the early components of the visual evoked potential. *Hum Brain Mapp* **15**: 95–111.

Farrant M, Nusser Z (2005). Variations on an inhibitory theme: phasic and tonic activation of GABA(A) receptors. *Nat Rev Neurosci* **6**: 215–229.

Fink-Jensen A, Suzdak PD, Swedberg MD, Judge ME, Hansen L, Nielsen PG (1992). The gamma-aminobutyric acid (GABA) uptake inhibitor, tiagabine, increases extracellular brain levels of GABA in awake rats. *Eur J Pharmacol* **220**: 197–201.

Frankle WG, Cho RY, Mason NS, Chen CM, Himes M, Walker C *et al* (2012). [11C]flumazenil binding is increased in a dose-dependent manner with tiagabine-induced elevations in GABA levels. *PLoS One* **7**: e32443.

Frankle WG, Cho RY, Narendran R, Mason NS, Vora S, Litschge M *et al* (2009). Tiagabine increases [11C]flumazenil binding in cortical brain regions in healthy control subjects. *Neuropsychopharmacology* **34**: 624–633.

Fries P, Scheeringa R, Oostenveld R (2008). Finding gamma. *Neuron* **58**: 303–305.

Hall SD, Barnes GR, Furlong PL, Seri S, Hillebrand A (2010). Neuronal network pharmacodynamics of GABAergic modulation in the human cortex determined using pharmaco-magnetoencephalography. *Hum Brain Mapp* **31**: 581–594.

Hendry SH, Huntsman MM, Vinuela A, Mohler H, de Blas AL, Jones EG (1994). GABAA receptor subunit immunoreactivity in primate visual cortex: distribution in macaques and humans and regulation by visual input in adulthood. *J Neurosci* **14**: 2383–2401.

Hillebrand A, Singh KD, Holliday I, Furlong PL, Barnes GR (2005). A new approach to neuroimaging with magnetoencephalography. *Hum Brain Mapp* **25**: 199–211.

Hoogenboom N, Schoffelen JM, Oostenveld R, Fries P (2010). Visually induced gamma-band activity predicts speed of change detection in humans. *Neuroimage* **51**: 1162–1167.

Huang MX, Mosher JC, Leahy RM (1999). A sensor-weighted overlapping-sphere head model and exhaustive head model comparison for MEG. *Phys Med Biol* **44**: 423–440.

Jenkinson M, Smith S (2001). A global optimisation method for robust affine registration of brain images. *Med Image Anal* **5**: 143–156.

Kahlbrock N, Butz M, May ES, Schnitzler A (2012). Sustained gamma band synchronization in early visual areas reflects the level of selective attention. *Neuroimage* **59**: 673–681.

Katzner S, Busse L, Carandini M (2011). GABAA inhibition controls response gain in visual cortex. *J Neurosci* **31**: 5931–5941.

Kraut MA, Arezzo JC, Vaughan Jr HG (1985). Intracortical generators of the flash VEP in monkeys. *Electroencephalogr Clin Neurophysiol* **62**: 300–312.

Le Van Quyen M, Foucher J, Lachaux JP, Rodriguez E, Lutz A, Martinerie J *et al* (2001). Comparison of Hilbert transform and wavelet methods for the analysis of neuronal synchrony. *J Neurosci Methods* **111**: 83–98.

Loughnan BL, Sebel PS, Thomas D, Rutherfoord CF, Rogers H (1987). Evoked potentials following diazepam or fentanyl. *Anaesthesia* **42**: 195–198.

Martin CS, Earleywine M, Musty RE, Perrine MW, Swift RM (1993). Development and validation of the biphasic alcohol effects scale. *Alcohol Clin Exp Res* **17**: 140–146.

Minelli A, Brecha NC, Karschin C, DeBiasi S, Conti F (1995). GAT-1, a high-affinity GABA plasma membrane transporter, is localized to neurons and astroglia in the cerebral cortex. *J Neurosci* **15**: 7734–7746.

Mody I, De Koninck Y, Otis TS, Soltesz I (1994). Bridging the cleft at GABA synapses in the brain. *Trends Neurosci* **17**: 517–525.

Muthukumaraswamy SD (2010). Functional properties of human primary motor cortex gamma oscillations. *J Neurophysiol* **104**: 2873–2885.

Muthukumaraswamy SD, Edden RAE, Jones DK, Swettenham JB, Singh KD (2009). Resting GABA concentration predicts peak gamma frequency and fMRI amplitude in response to visual stimulation in humans. *Proc Natl Acad Sci USA* **106**: 8356–8361.

Muthukumaraswamy SD, Singh KD, Swettenham JB, Jones DK (2010). Visual gamma oscillations and evoked responses: variability, repeatability and structural MRI correlates. *NeuroImage* **49**: 3349–3357.

Myers JF, Stokes PRA, Kalk NJ, Watson BJ, Erritzoe D, Wilson SJ *et al* (2012). Sensitivity of the benzodiazepine inverse agonist PET ligand [11C]Ro15-4513 to changes in endogenous GABA. *J Cereb Blood Flow Metab* **32**: S1:P069.

Olivas ND, Quintanar-Zilinskas V, Nenadic Z, Xu X (2012). Laminar circuit organization and response modulation in mouse visual cortex. *Front Neural Circuits* **6**: 70.

Pelli DG (1997). The VideoToolbox software for visual psychophysics: transforming numbers into movies. *Spat Vis* **10**: 437–442.

Perry G, Adjamian P, Thai NJ, Holliday IE, Hillebrand A, Barnes GR (2011). Retinotopic mapping of the primary visual cortex – a challenge for MEG imaging of the human cortex. *Eur J Neurosci* **34**: 652–661.

Puts NA, Edden RA (2012). In vivo magnetic resonance spectroscopy of GABA: a methodological review. *Prog Nucl Magn Reson Spectrosc* **60**: 29–41.

Restuccia D, Valeriani M, Grassi E, Gentili G, Mazza S, Tonali P *et al* (2002). Contribution of GABAergic cortical circuitry in shaping somatosensory evoked scalp responses: specific changes after single-dose administration of tiagabine. *Clin Neurophysiol* **113**: 656–671.

Robinson SE (ed) (2004). Localization of event-related activity by SAM(erf). *Biomag 2004: Proceedings of the 14th International Conference on Biomagnetism. Boston, USA*. Biomag 2004: Boston, USA.

Robinson SE, Vrba J (1999). Functional neuroimaging by synthetic aperture manetometry (SAM). In: Yoshimoto TKotani MKuriki SKaribe HNakasato N (eds) *Recent Advances in Biomagnetism*. Tohoku University Press: Sendai, pp 302–305.

Roepstorff A, Lambert JD (1994). Factors contributing to the decay of the stimulus-evoked IPSC in rat hippocampal CA1 neurons. *J Neurophysiol* **72**: 2911–2926.

Schuckit MA (1980). Self-rating of alcohol intoxication by young men with and without family histories of alcoholism. *J Stud Alcohol* **41**: 242–249.

Schwarzkopf DS, Robertson DJ, Song C, Barnes GR, Rees G (2012). The frequency of visually induced gamma-band oscillations depends on the size of early human visual cortex. *J Neurosci* **32**: 1507–1512.

Smith SM (2002). Fast robust automated brain extraction. *Hum Brain Mapp* **17**: 143–155.

Swettenham JB, Muthukumaraswamy SD, Singh KD (2009). Spectral properties of induced and evoked gamma oscillations in human early visual cortex to moving and stationary stimuli. *J Neurophysiol* **102**: 1241–1253.

Thompson SM, Gahwiler BH (1992). Effects of the GABA uptake inhibitor tiagabine on inhibitory synaptic potentials in rat hippocampal slice cultures. *J Neurophysiol* **67**: 1698–1701.

Traub RD, Whittington MA, Colling SB, Buzsaki G, Jefferys JGR (1996). Analysis of gamma rhythms in the rat hippocampus in vitro and in vivo. *J Physiol-London* **493**: 471–484.

van Leeuwen TH, Verbaten MN, Koelega HS, Kenemans JL, Slangen JL (1992). Effects of bromazepam on single-trial event-related potentials in a visual vigilance task. *Psychopharmacology (Berl)* **106**: 555–564.

Vrba J, Robinson SE (2001). Signal processing in magnetoencephalography. *Methods* **25**: 249–271.

Whitham EM, Lewis T, Pope KJ, Fitzgibbon SP, Clark CR, Loveless S *et al* (2008). Thinking activates EMG in scalp electrical recordings. *Clin Neurophysiol* **119**: 1166–1175.

Whitham EM, Pope KJ, Fitzgibbon SP, Lewis T, Clark CR, Loveless S *et al* (2007). Scalp electrical recording during paralysis: quantitative evidence that EEG frequencies above 20 Hz are contaminated by EMG. *Clin Neurophysiol* **118**: 1877–1888.

Xing D, Yeh CI, Burns S, Shapley RM (2012). Laminar analysis of visually evoked activity in the primary visual cortex. *Proc Natl Acad Sci USA* **109**: 13871–13876.

Yuval-Greenberg S, Keren AS, Tomer O, Nelken I, Deouell LY (2009). Response to Letter: Melloni et al., "Transient induced gamma-band response in EEG as a manifestation of miniature saccades." Neuron 58, 429–441. *Neuron* **62**: 10–12.

Yuval-Greenberg S, Tomer O, Keren AS, Nelken I, Deouelll LY (2008). Transient induced gamma-band response in EEG as a manifestation of miniature saccades. *Neuron* **58**: 429–441.

Zilles K, Palomero-Gallagher N, Schleicher A (2004). Transmitter receptors and functional anatomy of the cerebral cortex. *J Anat* **205**: 417–432.